The International Journal of Advanced Manufacturing Technology
https://doi.org/10.1007/s00170-023-12866-0

ORIGINAL ARTICLE

Enhanced investigations and modeling of surface roughness of epoxy/Alfa fiber biocomposites using optimized neural network architecture with genetic algorithms

Madani Grine[1,2] · Mohamed Slamani[1,2,3] · Aissa Laouissi[4] · Mustapha Arslane[1] · Mansour Rokbi[2] · Jean-François Chatelain[3]

Received: 28 July 2023 / Accepted: 11 December 2023

Abstract
Currently, there is a notable attraction within the industry towards biocomposites, driven by the increasing fascination with natural fiber-reinforced composites (NFRCs). These NFRCs offer remarkable benefits, including cost-effectiveness, biodegradability, eco-friendliness, and favorable mechanical properties. As a result, the manufacturing processes of natural fiber reinforced polymer (NFRP) composites have garnered attention from both industrial professionals and scientists. The emergence of these eco-friendly materials in the automotive and aerospace industries has sparked interest in understanding their production techniques. However, the machining processes of NFRP composites pose significant challenges due to the complex structure of natural fibers, necessitating thorough studies to address these issues effectively. This research paper presents a comprehensive investigation on surface roughness during the milling process of Alfa/epoxy biocomposites. A set of 100 experimental trials was conducted to test the surface roughness, and analysis of variance (ANOVA) was used to assess the impact of cutting parameters and chemical treatment on surface quality.
To develop a predictive model for surface roughness, a hybrid approach called ANN-GA (artificial neural networks-genetic algorithms) is proposed in this research. This approach combines ANN and GA to determine an optimal neural network architecture. The performance of the ANN-GA model is compared to the Levenberg–Marquardt backpropagation (LM) algorithm. ANOVA results show that the feed per revolution have a significant influence on surface roughness, followed by the chemical treatment of fibers, while machining direction has a smaller effect. The ANN-GA model demonstrates good accuracy in surface roughness prediction compared to the LM algorithm.

Keywords Biocomposite · Alfa fibers · Surface roughness · Optimization · ANN · GA

1 Introduction

Natural fiber composites have emerged as a viable alternative to traditional materials in various lightweight structural applications. The integration of plant fibers as reinforcement in composites offers remarkable advantages in terms of attractive physical and mechanical properties, such as low cost, high wear resistance, light weight, and potential for substitution for many conventional materials [1, 2]. However, in order to enhance market acceptance of these materials, additional characteristics need to be investigated. Plant fiber-reinforced composites have found applications in the interior components of various car brands [3, 4], marine vessels [5, 6], and construction sector for secondary structures, addressing concerns regarding environmental conservation [7, 8]. While composite

✉ Mohamed Slamani
mohamed.slamani@univ-msila.dz

1 MMS Lab, Faculty of Technology, University of M'sila, M'sila, Algeria

2 Mechanical Engineering Department, Faculty of Technology, University of M'sila, M'sila, Algeria

3 Mechanical Engineering Department, École de Technologie Supérieure, Montreal, Canada

4 Mechanics Research Centre, Po, Box 73B, 25000 Constantine, Algeria

Published online: 28 December 2023

materials are relatively easier to process during mold production, machining is still necessary for repair and assembly purposes. The machining of composites is influenced by factors such as fiber orientation, nature, size, and cutting conditions, which significantly impact machinability, cutting forces, and the quality of machined surfaces [9–12]. It is widely acknowledged in the field that prior to utilizing composites reinforced with natural fibers, it is crucial to subject these fibers to a pretreatment process. Among the various effective methods for enhancing the properties of natural fibers, alkaline treatment is extensively employed to eliminate certain impurities present on the surface, such as hemicelluloses, lignin, pectin, and wax [13]. As a result, the fibers' surface becomes more uniform through impurity removal, leading to improved stress transfer efficiency and adhesion properties between the fiber and the matrix [14]. However, despite the well-established benefits of alkali treatment on fiber characteristics, its impact on surface roughness during machining has yet to be thoroughly investigated.

Alfa fibers, derived naturally and biodegradable, represent cost-effective materials readily accessible in Algeria, with substantial annual production in North Africa and Spain. Flourishing without the need for insecticides or pesticides and requiring minimal water, Alfa grass is a perennial plant that endures throughout the seasons [15]. Algeria, a major Alfa producer, cultivates approximately 4 million hectares of this abundant wild herb, renowned for its eco-friendly and cost-effective attributes [16]. Comprising cellulose, hemicellulose, lignin, and ash [16], the biochemical composition of Alfa may slightly vary depending on climatic and soil conditions, falling within the ranges (dry weight) of 48–63%, 9–22%, and 12–18%, respectively [16–19]. Its high polysaccharide concentration gives Alfa significant potential as a raw material for bioethanol production [20]. Studies confirm that these plants are chemically inert [21], with no reported dermatological or respiratory reactions during harvesting or fabrication, eliminating the need for special protective equipment [22].

Predominantly employed in paper production, these fibers have recently found application as reinforcement in the production of biodegradable composites [23, 24] and are now being used in diverse fields such as packaging, construction, aerospace, and the automotive industry [25].

In exploring the benefits of Alfa fibers, researchers have delved into volume fractions, orientations of Alfa fibers [15, 26], and the replacement of glass fibers in composite materials [27]. Investigations into the effects of chemical treatments on mechanical and permeability properties have been conducted [28, 29], revealing favorable characteristics in the mechanical behavior of polypropylene reinforced with Alfa fibers [30, 31]. Alfa fibers can be effectively combined with a matrix and supplementary materials as a hybrid composite [32, 33]. Recent research has focused on assessing the feasibility of using Alfa fibers as reinforcement for polymer composites [26, 31, 34].

Conversely, in recent years, numerous studies have focused on examining the influence of cutting parameters on the machinability of natural fiber composites. These investigations have employed regression analysis and artificial intelligence techniques to reduce the number of experiments, identify optimal cutting conditions, and develop predictive models with acceptable accuracy. However, the quantity of such studies remains relatively limited when compared to research conducted on machining synthetic fiber reinforced composites.

In their research, Chegdani et al. [35, 36] explored the impact of flax fiber orientation on the machinability and surface quality of polypropylene polymer composites reinforced with unidirectional flax fibers. The findings indicate that fiber orientation plays a significant role in determining the quality of machined surfaces. Specifically, a fiber orientation of $\theta = 45°$ demonstrated the most favorable machinability and resulted in the lowest surface roughness.

Kumaran et al. [37] used regression analysis to predict the surface roughness when machining two unidirectional and unidirectional carbon fiber reinforced plastics with abrasive water jet woven fabric surface. The experimental results yielded quadratic models for the roughness parameter Ra, which demonstrated high accuracy with R^2 values of 96.03% and 93.22% for the respective materials.

John et al. [38] conducted an experimental study to examine the impact of cutting parameters on the surface finish of end-milled polypropylene composites reinforced with jute and kenaf fibers. The results revealed that the quality of the machined surfaces is predominantly influenced by the spindle speed, which has a contribution three times greater than the feed rate.

Vinayagamoorthy and Rajeswari [39] investigated the machinability of a recently developed composite material composed of an isophthalic polyester matrix reinforced with natural jute fibers. The material was milled using an HSS cutter, and the researchers found that the cutting speed and depth of cut were the primary factors affecting the pushing force. Additionally, they determined that the

depth of cut had the most significant impact on the torque generated during the milling process.

Babu et al. [40] examined the machining parameters and the impact of different fiber reinforcements (jute, kenaf, fiberglass, and banana) on surface roughness (Ra) and delamination factor (Fd) during the end milling process of composites. The findings revealed that the feed rate and cutting speed were the primary factors influencing Fd and Ra. It was observed that employing a high cutting speed and a low feed rate is favorable for enhancing surface quality and reducing delamination. Similar conclusions were drawn by Harun et al. [41] when investigating the milling of composites reinforced with kenaf fibers.

Benyettou et al. [42] have devised a mathematical model employing artificial neural networks (ANN) to forecast delamination values in the drilling process of biocomposites reinforced with cellulosic fibers. The resulting ANN model demonstrates outstanding accuracy, boasting an R^2 value of 0.98.

Tran et al. [43] investigated the impact of cutting parameters and reinforcement type on the machinability of biocomposites comprising PP reinforced with chopped miscanthus fibers (M2) and biocarbon particles (M1) using the RSM method. The analysis of variance (ANOVA) revealed that spindle speed exerted the greatest influence on surface roughness (Ra), with Fisher values (F) of 100.22 and 15.28 for M1 and M2, respectively. The drill diameter followed closely with F values of 91.65 and 30.78 for M1 and M2, respectively. The mathematical prediction models generated by RSM displayed a satisfactory correlation for M1, with $R^2 = 92.1\%$, and a weaker correlation for M2, with $R^2 = 74.1\%$. In a separate study [44], the same researchers found that modeling Ra using the ANFIS approach yielded superior predictive accuracy compared to linear regression models when examining three novel PP-matrix biocomposites.

Belaadi et al. [45] have conducted a comprehensive study utilizing a hybrid RSM-ANN-GA optimization approach. They employed the results obtained from a complete factorial plan L27 to analyze the impact of drilling parameters on the delamination factor (Fd) and to both model and optimize Fd. The study demonstrated remarkable concurrence between the experimental results and those estimated using RSM and ANN. The optimization results obtained through GA and DF approaches were highly similar, leading to the identification of the optimal drilling regime with parameters set at $f = 50$ mm/min, $N = 806$ rpm, and $d = 5$ mm.

The primary objective of this study is to thoroughly investigate and analyze the surface roughness that arises during the trimming process of Alfa fiber-reinforced epoxy-based biocomposites.

This research primarily focuses on the distinctive application of natural fiber-reinforced composites (NFRCs) as a compelling alternative to conventional metals and synthetic fiber-reinforced composites. By thoroughly exploring and analyzing the surface roughness characteristics of NFRCs, this study seeks to make a substantial contribution to the understanding and advancement of biocomposites as a highly promising material option across various industries.

The novelty and innovation of this work are multifaceted. Firstly, it addresses the rapidly growing interest and increasing allure surrounding biocomposites, particularly natural fiber-reinforced composites (NFRCs), within the industry. By concentrating specifically on the surface roughness of Alfa/epoxy biocomposites, this study delves into a niche application of NFRCs in manufacturing processes that has received relatively little attention thus far.

Secondly, the comprehensive investigation undertaken to examine the surface roughness during the milling process of Alfa/epoxy biocomposites significantly contributes to our understanding of the production techniques involved in manufacturing these environmentally friendly materials. It provides invaluable insights into the impact of cutting parameters and chemical treatments, such as alkali treatment with NaOH, on surface quality, which is crucial for optimizing the machining processes associated with NFRCs.

Moreover, the study introduces an innovative hybrid approach known as ANN-GA (artificial neural networks-genetic algorithms) for the accurate prediction of surface roughness. By leveraging the strengths of artificial neural networks and genetic algorithms, optimal neural network architecture is developed specifically to predict surface roughness with exceptional precision in the context of Alfa/epoxy biocomposites.

The comparison between the performance of the ANN-GA model and the widely employed Levenberg–Marquardt backpropagation algorithm further underscores the originality and significance of this study. The results unequivocally demonstrate the superior predictive capabilities of the ANN-GA model, thereby showcasing the immense potential of this hybrid approach in augmenting the accuracy of surface roughness predictions.

In summary, this research constitutes a distinctive and highly valuable contribution to the field by

comprehensively investigating the surface roughness of NFRCs, employing the innovative ANN-GA hybrid approach, and conducting a meticulous evaluation of its performance in comparison to conventional algorithms. The invaluable findings and insights derived from this study have the potential to facilitate further advancements in the manufacturing and optimization of biocomposites, with a particular focus on enhancing surface quality. Furthermore, it sheds new light on the significance of pre-treating natural fibers, such as Alfa fibers, through alkali treatment with NaOH, and its potential implications on surface roughness during the machining process of biocomposites.

2 Test methods and materials

2.1 Experimental materials

In this study, two epoxy biocomposite panels were fabricated and analyzed. One panel was reinforced with treated Alfa fibers, while the other panel was reinforced with untreated Alfa fibers.

The extraction process of the natural fibers from the Alfa plant involved several steps. First, the fibers were soaked in water for 25 days, after which they were extracted and placed in an oven at a temperature of 70°C for 6 h in the case of untreated fibers. For the treated fibers, a chemical treatment was performed using a 5% NaOH alkaline solution to remove lignin, wax, and impurities from the outer surface of the fibers. Subsequently, the fibers were immersed in a 2% sulfuric acid (H_2SO_4) solution for 2 min to halt the reaction between the Alfa sheets and the soda, thereby preventing degradation of the cellulosic material. The fibers were then rinsed multiple times with distilled water, with the pH of the Alfa leaves checked after each rinse. The goal was to reach a neutral pH (pH = 7) to eliminate any remaining traces of the NaOH solution from the fibers. Finally, the fibers were manually woven into unidirectional plies with a basis weight of 600 g/m^2, forming four-layer plate measuring $250 \times 250 \times 10$ mm^3. This plate was obtained through a vacuum molding process (Fig. 1).

Following that, biocomposite plates (Alfa/epoxy) were manufactured with a fiber content of 40% by weight. The selected matrix was MEDAPOXY STR brand epoxy resin, characterized by a viscosity of 11000 MPa.s at 25°C and a density of 1.1 ± 0.05.

Vacuum casting was employed to create the plates, utilizing four identical layers, each measuring 2 mm in thickness. Subsequently, the samples were placed in an oven set to a temperature of 70°C for duration of 12 h to ensure complete curing.

The trimming operations were conducted utilizing a PEARL RIVER NC F-VMC 510L machining center, which is a three-axis numerically controlled machine tool (MOCN) equipped with a SIEMENS 840D controller.

To ensure safety during machining, a machining jig was securely fastened to the machine table, featuring pre-grooves to prevent any collision between the tool end and the jig. For the trimming process, a super high-speed steel (HSS-SUPER) milling cutter with four teeth, a diameter of 10 mm, and a helix angle of 30° were employed. The total length of the milling cutter is 70 mm. Following the completion of the machining, the surface roughness of the machined profiles under different machining conditions was measured using a PCE_RT1200 model roughness meter.

2.2 Design of experiments

In this research, a comprehensive factorial design comprising 5^2 combinations was implemented, resulting in a total of 25 experimental tests conducted on both treated and untreated plaques. The factors of interest in this investigation were cutting velocity (Vc) and feed per revolution (f), which are fundamental parameters in the machining process. The primary aim of this study was to assess the machining behavior of biocomposites in terms of surface roughness, considering both untreated (UT) and treated fibers (T).

The factorial design allows for the systematic exploration of various combinations of cutting velocity and feed per revolution, enabling a comprehensive analysis of their influence on the machining process. This design approach ensures that all possible combinations are considered, providing a robust understanding of the factors' effects.

Table 1 presents the specific input factors and their corresponding levels used in the experimental design. The cutting velocity is varied at different levels, as well as the feed per revolution, to capture the range of operating conditions encountered in practical machining scenarios. By systematically varying these factors and observing their impact on the machining behavior, valuable insights can be gained regarding the optimal machining parameters for biocomposites.

To examine the effects of the factors under investigation, each composite plate was subjected to cutting along two directions: parallel to the fiber direction 0° and perpendicular to it 90°. This arrangement allowed for a total of 50 cutting sides per plate. Figure 2 presents a schematic

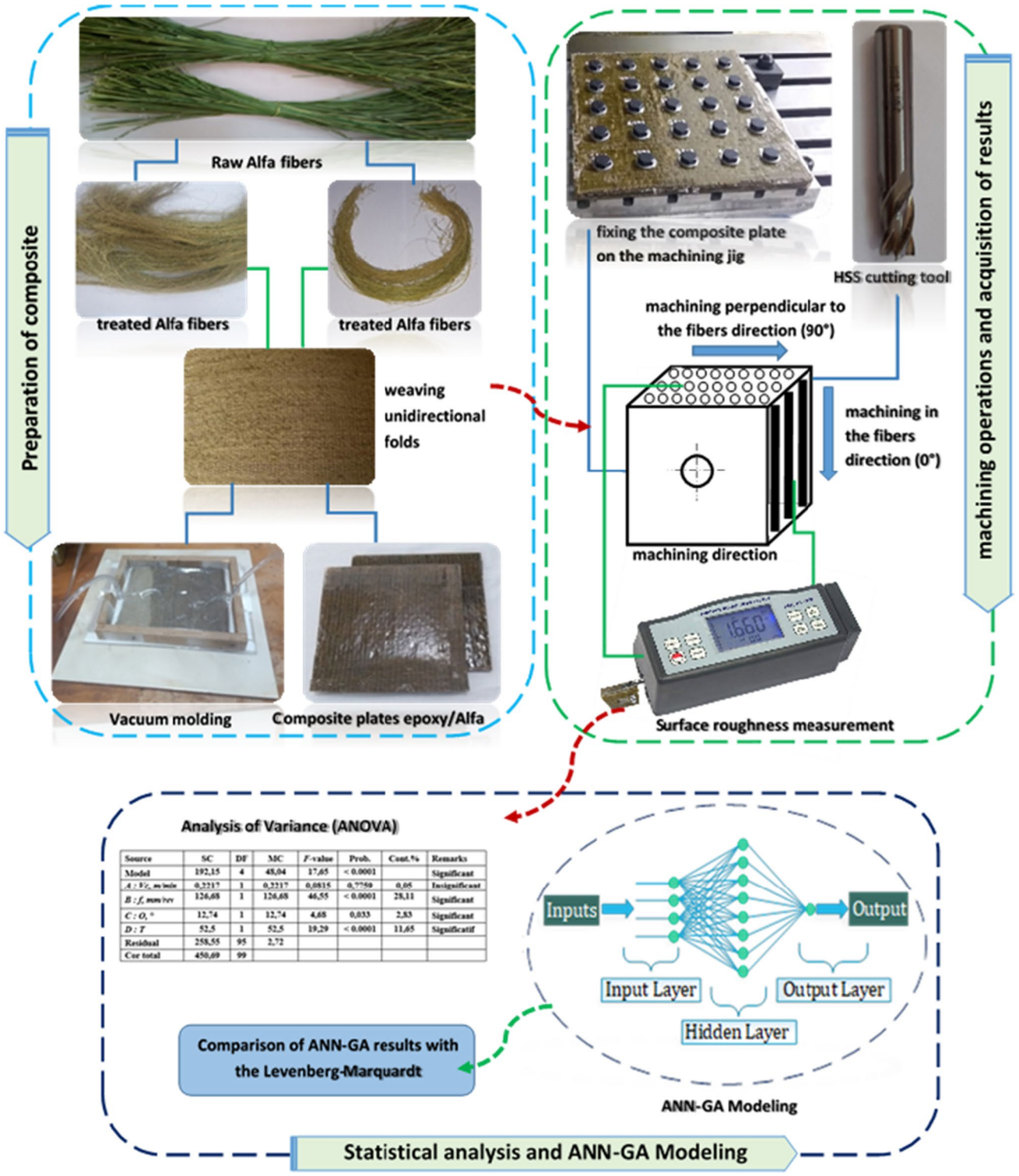

Fig. 1 Overview of experimental procedures

representation of one of the 25 trimmed specimens, highlighting the cutting sides. It is noteworthy that each coupon represented a maximum of four distinct experimental combinations, comprising one combination per side, including two combinations involving down milling and two involving up milling. Consequently, a total of 100 machined

Table 1 Input factors and their corresponding levels used in the experimental design

Level	*Vc* (m/min)	*f* (mm/rev)	Treatment *(Tr)*	*Fibre orientation (O°)*
1	50	0.05	UT	0°
2	100	0.15	T	90°
3	150	0.25	-	-
4	200	0.4	-	-
5	225	0.5	-	-

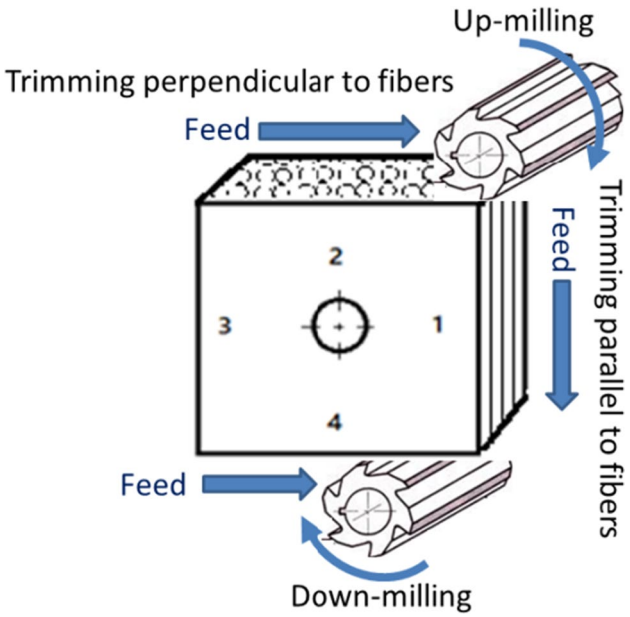

Fig. 2 Cutting sides and associated cutting conditions for each coupon

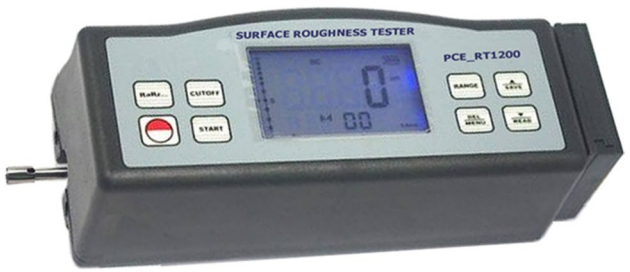

Fig. 3 PCE RT 1200 Profilometer Surface Roughness Tester

sides were obtained, considering the combinations of treated and untreated plaques, as well as the up milling and down milling approaches (25 coupons × 4 sides).

Following the machining process, meticulous cleaning was conducted on all machined sides to eliminate impurities and dust. This was achieved by employing blown compressed air. Subsequently, the surface roughness, specifically the roughness average (Ra), of each side of every coupon, representing each cutting condition, was measured. To carry out these measurements, a PCE RT 1200 Profilometer Surface Roughness Tester (Fig. 3) equipped with a probe having a diameter of 5 µm and an orientation of 90° with respect to the surfaces was utilized.

3 Results and discussion

The cutting conditions (cutting velocity Vc and the feed per revolution f), the nature of treatment (treated and untreated), the fibers orientation (O), and the corresponding experimental results for surface roughness (Ra) of the 100 machined profiles, based on the complete factorial design, are displayed in Table 2.

3.1 Analysis of variance (ANOVA)

The analysis of variance (ANOVA) is a statistical method employed to examine the relationship between one or more input variables and a target variable, known as the output. It is also used to classify these input variables based on their effects on the output variable [46]. Table 3 displays the ANOVA results for Ra. The analysis is conducted at a significance level of $\alpha = 0.05$, corresponding to a 95% confidence level. A low probability value (≤ 0.05) or 95% confidence level indicates the obtained models are statistically significant, which is desirable.

The ANOVA table for Ra includes the degrees of freedom (DoF), sum of squares (SS), mean squares (MS), probability (Prob.), and percentage contribution (Cont. %) of each tested factor.

By closely examining the Ra values in Table 2 and the ANOVA results presented in Table 3, we can rank the cutting parameters (Vc and f), fiber orientation, and fiber treatment based on their influence on surface roughness. The feed per revolution (f) emerges as the most influential factor (28.11%), to the surface roughness, with a noticeable impact as it increases. Fiber treatment is also significant, with an impact of 11.65%. Fiber orientation has a discernible effect of 2.83%. Cutting velocity, on the other hand, does not exhibit a significant influence on surface roughness.

Figures 4a and b depicts the three-dimensional (3D) response surfaces showcasing the relationship between

Table 2 Design of experiments (DOE) and experimental results of surface roughness (Ra)

	Input factors (coded values)				Output factors	Input factor (coded values)					Output factors
N°	*Vc (m/min)*	*f (mm/rev)*	*O (°)*	*Tr*	*Ra (µm)*	N°	*Vc (m/min)*	*f (mm/rev)*	*O (°)*	*Tr*	*Ra (µm)*
1	50	0.05	0	UT	4.06	51	50	0.05	90	UT	11.83
2	100	0.05	0	UT	3.96	52	100	0.05	90	UT	10.43
3	150	0.05	0	UT	2.66	53	150	0.05	90	UT	8.3
4	200	0.05	0	UT	5.36	54	200	0.05	90	UT	10.5
5	225	0.05	0	UT	5.76	55	225	0.05	90	UT	7.5
6	50	0.15	0	UT	2.16	56	50	0.15	90	UT	4.86
7	100	0.15	0	UT	1.6	57	100	0.15	90	UT	2.7
8	150	0.15	0	UT	1.66	58	150	0.15	90	UT	3
9	200	0.15	0	UT	2.9	59	200	0.15	90	UT	4.56
10	225	0.15	0	UT	3.76	60	225	0.15	90	UT	4.66
11	50	0.25	0	UT	1.96	61	50	0.25	90	UT	2.86
12	100	0.25	0	UT	2.13	62	100	0.25	90	UT	4.86
13	150	0.25	0	UT	2.53	63	150	0.25	90	UT	2.7
14	200	0.25	0	UT	2	64	200	0.25	90	UT	2.13
15	225	0.25	0	UT	3.7	65	225	0.25	90	UT	2.33
16	50	0.4	0	UT	2.6	66	50	0.4	90	UT	1.86
17	100	0.4	0	UT	2.33	67	100	0.4	90	UT	3.13
18	150	0.4	0	UT	2.4	68	150	0.4	90	UT	4.66
19	200	0.4	0	UT	2.63	69	200	0.4	90	UT	2.43
20	225	0.4	0	UT	1.8	70	225	0.4	90	UT	2.83
21	50	0.5	0	UT	1.96	71	50	0.5	90	UT	3.53
22	100	0.5	0	UT	2.8	72	100	0.5	90	UT	2.76
23	150	0.5	0	UT	2.3	73	150	0.5	90	UT	2.6
24	200	0.5	0	UT	2.33	74	200	0.5	90	UT	4.3
25	225	0.5	0	UT	2.4	75	225	0.5	90	UT	2.63
26	50	0.05	0	T	11.83	76	50	0.05	90	T	11.83
27	100	0.05	0	T	10.43	77	100	0.05	90	T	10.43
28	150	0.05	0	T	8.3	78	150	0.05	90	T	8.3
29	200	0.05	0	T	10.5	79	200	0.05	90	T	10.5
30	225	0.05	0	T	7.5	80	225	0.05	90	T	7.5
31	50	0.15	0	T	4.86	81	50	0.15	90	T	4.86
32	100	0.15	0	T	2.7	82	100	0.15	90	T	2.7
33	150	0.15	0	T	3	83	150	0.15	90	T	3
34	200	0.15	0	T	4.56	84	200	0.15	90	T	4.56
35	225	0.15	0	T	4.66	85	225	0.15	90	T	4.66
36	50	0.25	0	T	2.86	86	50	0.25	90	T	2.86
37	100	0.25	0	T	4.86	87	100	0.25	90	T	4.86
38	150	0.25	0	T	2.7	88	150	0.25	90	T	2.7
39	200	0.25	0	T	2.13	89	200	0.25	90	T	2.13
40	225	0.25	0	T	2.33	90	225	0.25	90	T	2.33
41	50	0.4	0	T	1.86	91	50	0.4	90	T	1.86
42	100	0.4	0	T	3.13	92	100	0.4	90	T	3.13
43	150	0.4	0	T	4.66	93	150	0.4	90	T	4.66
44	200	0.4	0	T	2.43	94	200	0.4	90	T	2.43
45	225	0.4	0	T	2.83	95	225	0.4	90	T	2.83
46	50	0.5	0	T	3.53	96	50	0.5	90	T	3.53
47	100	0.5	0	T	2.76	97	100	0.5	90	T	2.76

Table 2 (continued)

	Input factors (coded values)				Output factors	Input factor (coded values)					Output factors
N°	*Vc (m/min)*	*f (mm/rev)*	*O (°)*	*Tr*	*Ra (µm)*	N°	*Vc (m/min)*	*f (mm/rev)*	*O (°)*	*Tr*	*Ra (µm)*
48	150	0.5	0	T	2.6	98	150	0.5	90	T	2.6
49	200	0.5	0	T	11.83	99	200	0.5	90	T	4.3
50	225	0.5	0	T	10.43	100	225	0.5	90	T	2.63

Table 3 ANOVA for Ra

Source	SS	DoF	MS	*F*-value	Prob	Cont.%	Remarks
Model	192.15	4	48.04	17.65	< 0.0001		Significant
A: Vc, m/min	0.2217	1	0.2217	0.0815	0.7759	0.05	
B: f, mm/rev	126.68	1	126.68	46.55	< 0.0001	28.11	
C: O, °	12.74	1	12.74	4.68	0.033	2.83	
D: T	52.5	1	52.5	19.29	< 0.0001	11.65	
Residual	258.55	95	2.72				
Cor. total	450.69	99					

Ra and cutting velocity, feed per revolution, treatment, and fiber orientation. These surfaces validate the findings from the ANOVA analysis of Ra. It is evident that the feed per revolution exhibits the steepest slope, reinforcing its significant influence. The analysis of these surfaces reveals a substantial reduction in Ra with increasing feed per revolution. Conversely, the cutting velocity displays an almost negligible slope, indicating its negligible impact on surface roughness.

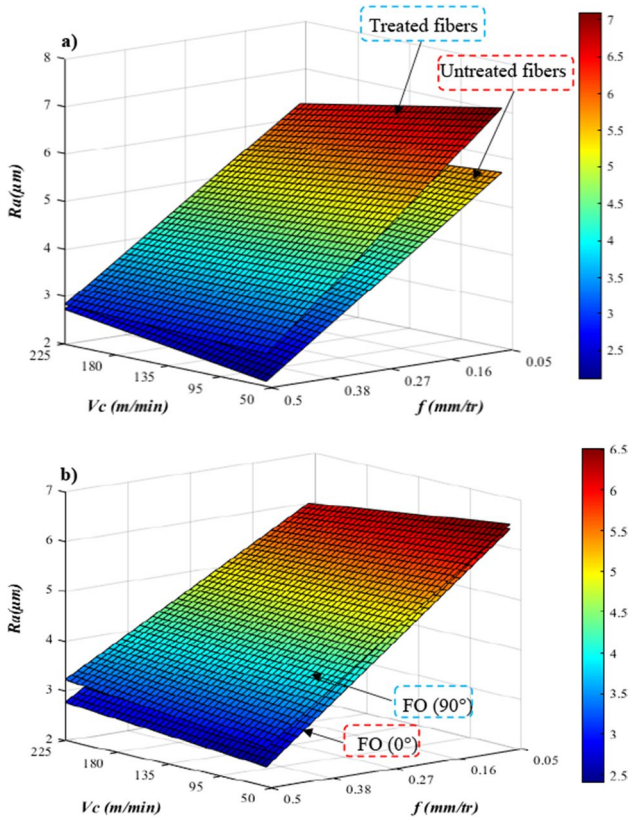

Fig. 4 3D response surfaces for Ra

Figure 4a shows that composites with untreated fibers exhibit superior surface quality compared to those with treated fibers, especially at low feed per revolution s. Alkaline treatment of Alfa fibers improves fiber interface quality matrix. Therefore, the adhesion of Alfa fibers treated with the polymer matrix is important (Benyahia, 2013) [47], which makes it more difficult to pull out the fibers when machining the Alfa/epoxy biocomposite. Hence, it results in reduced degradation of surface roughness.

Figure 4b illustrates the impact of fiber orientation on Ra. It is observed that the Ra values remain quite similar, with a slight improvement in surface roughness for biocomposites where the fibers are oriented at 0°, particularly at higher cutting velocity.

3.2 ANN-GA modeling

3.2.1 ANN modeling

In this study, the approach of artificial neural networks (ANN) is used to develop a predictive model of the surface roughness Ra as a function of the parameters studied in the previous part. ANN is a type of artificial intelligence technique that draws inspiration from the functioning of the

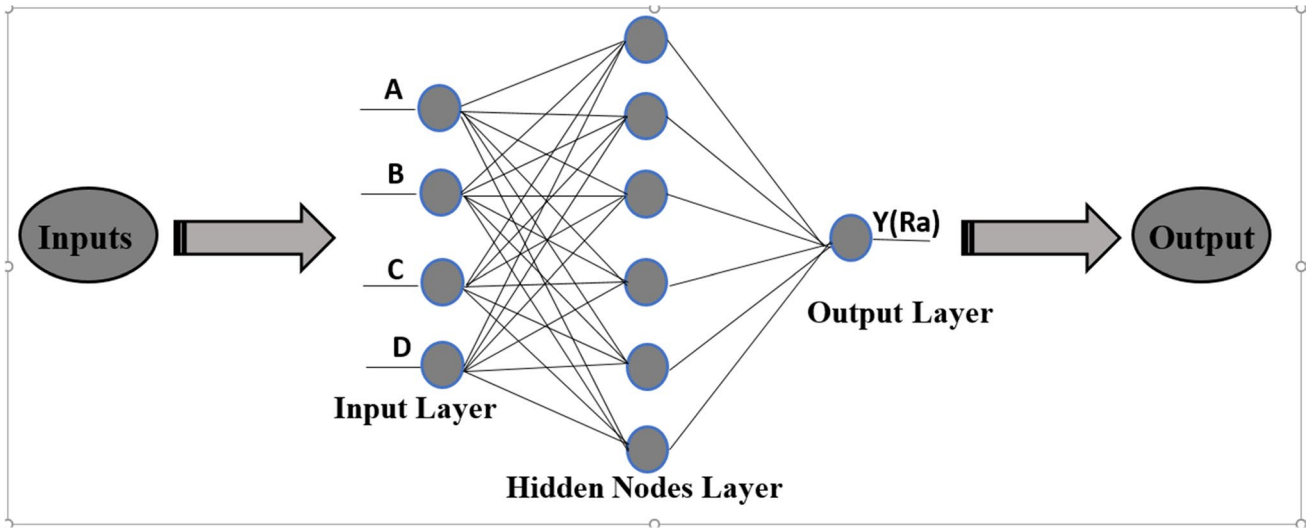

Fig. 5 Graphical representation of an ANN

human brain. They are capable of performing various valuable tasks in industrial applications, including modeling, classification, and data processing activities [48]. ANN consists of three types of layers: the input layer, the output layer, and potentially one or more hidden layers (as shown in Fig. 5) [49]. In a neural network with L + 1 layers, the following quantities are defined:

$$Z_j^l = \sum_k w_{jk} a_k^{l-1} + b_j^l, \forall l = 1, \ldots, L-1, L+1 \quad (1)$$

$$a_j^l = f\left(\sum_k w_{jk} a_k^{l-1} + b_j^l\right) = f\left(Z_j^l\right), \forall l = 1, \ldots, L-1, L+1 \quad (2)$$

Or $a_j^0 = x_j$ (x_j is here $j^{ième}$ input data), w_{jk}^l the weight value of the $k^{ième}$ neuron in the $(L-1)^{ième}$ layer at $j^{ième}$ neuron in the $l^{ième}$ layer, b_i^j are the biases and f is the activation function.

3.2.2 Learning a neural network

The learning problem boils down to minimizing an evaluation function, which evaluates the performance of a neural network on a set of data. The evaluation function depends on the adaptive parameters (bias and weight) of the neural network.

The learning problem for neural networks is formulated as finding a vector of parameters w_i and b_i for which the evaluation function f reaches a minimum value. The necessary condition states that if the neural network is at a minimum of the evaluation function.

A variety of algorithms are utilized to train neural networks, offering flexibility and diverse learning approaches. In this study, various optimization algorithms were employed to achieve an optimal architecture for the neural network: gradient descent (GD) [50–52], Newton's method (NM), gradient conjugué (CG) [53], quasi-Newton method (QNM), Levenberg–Marquardt (LM) algorithm [54], Bayesian regularization (BR) [55, 56], and genetic algorithms (GA) which are optimization algorithms based on techniques derived from genetics and natural evolution: crosses, mutations, and selection [57]. A genetic algorithm searches for the extrema or extrema of a function defined on a data space. Figure 6 illustrates the fundamental principle of how a genetic algorithm operates.

3.2.3 Optimization of a neural network "ANN" by genetic algorithms

a) **Presentation of the optimization algorithm of a neural network**

The present study utilized genetic algorithms to optimize the neural network architecture for a regression problem. The algorithm's principles can be summarized in the following steps:

1. The hyperparameters of the neural network to be optimized are defined, encompassing the number of layers, the number of neurons within each layer, the activation function assigned to each layer, the learning algorithm, and the iteration count for the learning process.
2. An evaluation endpoint is established to assess the quality of neural network predictions by comparing them with the actual values of the target variable. In this case, the evaluation endpoints include the coefficient of corre-

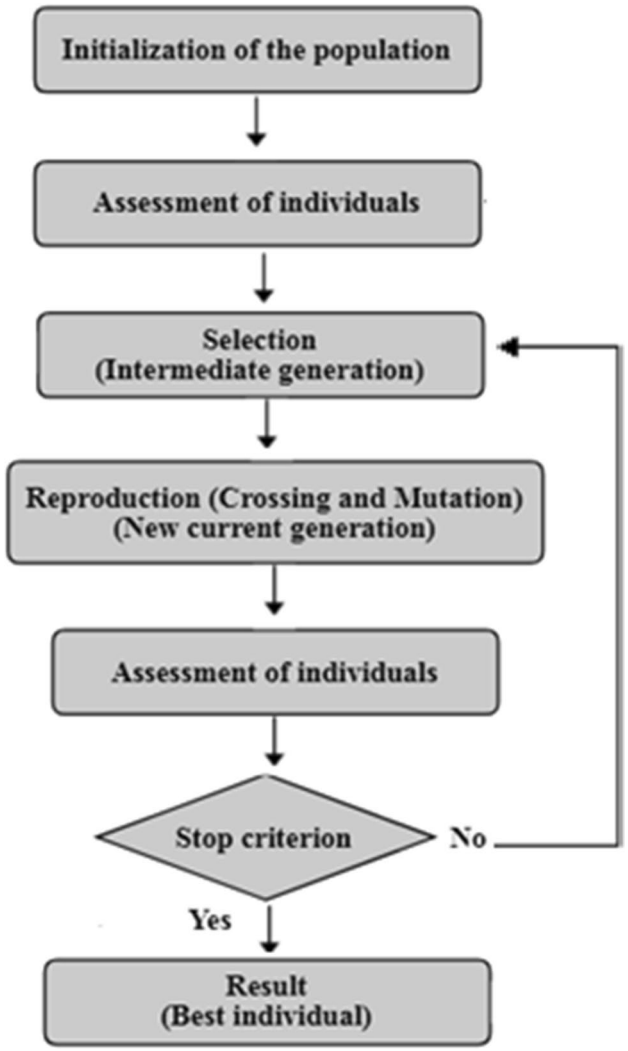

Fig. 6 Schematic diagram illustrating the fundamental principle of a genetic algorithm

Table 4 Evaluation criteria formulas

Criteria	Formulas
Mean absolute deviation	$MAD = \sum_{t=1}^{n} \frac{\lvert E_t - P_t \rvert}{n}$
Mean absolute percentage error (%)	$MAPE = \sum_{t=1}^{n} \frac{\lvert (E_t - P_t)/E_t \rvert}{n} \times 100$
Root mean square error	$RMSE = \sum_{t=1}^{n} \sqrt{\frac{(E_t - P_t)^2}{n}}$
Correlation coefficient	$R^2 = \frac{\sum_{t=1}^{n} (P_t - E_t)}{\sum_{t=1}^{n} (P_t - Y_e)^2}$

n the number of experience, E_t the experimental value of the ith experiment, P_t the predicted value of the ith experiment, Y_e the average response observed in the experiments

lation (R), root mean square error (RMSE), mean absolute deviation (MAD), mean absolute percentage error (MAPE), and mean absolute error (MAE). The formulas for calculating these different error criteria are presented in Table 4.

3. Define an initial population of random solutions, which represent different configurations of the neural network architecture and hyperparameters. Where 70% of the database was used to train the network and 20% for validation, 10% was used to test the accuracy of the obtained model.
4. The genetic operators, namely selection, crossover, and mutation, are applied to generate a new generation of solutions using the current population (adjust weights and bias of ANN).
5. Evaluate each next-gen solution using the rating function and select the best next-gen solutions (evaluate the generate ANN)
6. Steps 4 and 5 are repeated iteratively until an optimal solution is discovered or until a predefined stopping criterion is met.

After the genetic algorithm has converged to an optimal solution, the hyperparameters and optimal architecture of the neural network can be utilized to predict the values of the target variable (surface roughness Ra) on test data. The optimization method employed for the neural network architecture is summarized in a flowchart, depicted in Fig. 7. This visual representation encapsulates the various stages of the implemented optimization approach, providing a concise overview of the entire process.

b) **Optimization parameters**

The organization and connectivity of neurons in an artificial neural network are determined by its architecture. In this study, the parameters optimized were the network size, learning algorithm, and activation functions for each layer. The network size, which refers to the number of layers and nodes in each layer, is a crucial factor in neural network design. The learning algorithm is responsible for adjusting the weights and biases of the network to minimize prediction errors. Activation functions, on the other hand, determine the neuron's output based on its inputs.

To maximize network performance, the genetic algorithm was employed to optimize the network size, learning algorithm, and activation functions, aiming to identify the optimal combination of layers and nodes. Table 5 outlines the specific values utilized in this study

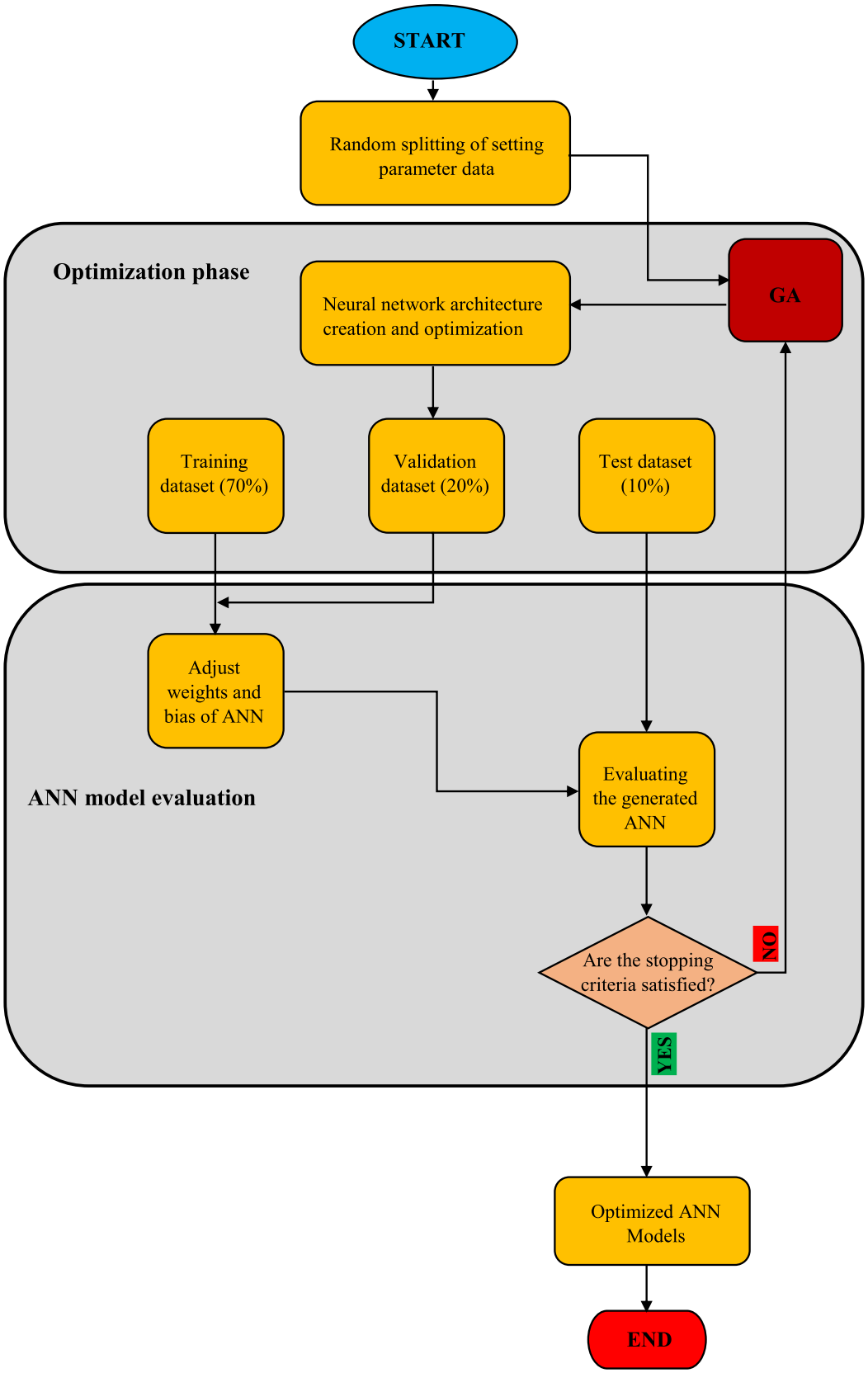

Fig. 7 Flowchart of optimization process based on ANN and GA

Table 5 ANN optimization parameters

Hidden layers	Hidden layer nodes	Learning algorithms	Activation functions
Min:1 Max:10	Min:1 Max:10	trainlm: Levenberg–Marquardt backpropagation	Compet: Competitive transfer function
		trainbr: Bayesian Regulation backpropagation	elliotsig: Elliot sigmoid transfer function
		trainbfg: BFGS quasi-Newton backpropagation	hardlim: Positive hard limit transfer function
		traincgb: Conjugate gradient backpropagation with Powell-Beale restarts	hardlims: Symmetric hard limit transfer function
		traincgf: Conjugate gradient backpropagation with Fletcher-Reeves updates	logsig: Logarithmic sigmoid transfer function
		traincgp: Conjugate gradient backpropagation with Polak-Ribiere updates	netinv: Inverse transfer function
		traingd: Gradient descent backpropagation	poslin: Positive linear transfer function
		traingda: Gradient descent with adaptive lr back-propagation	purelin: Linear transfer function
		traingdm: Gradient descent with momentum	radbas: Radial basis transfer function
		Traingdx: Gradient descent w/momentum & adaptive lr backpropagation	radbasn: Radial basis normalized transfer function
		trainoss: One step secant backpropagation	satlin: Positive saturating linear transfer function
		trainrp: RPROP backpropagation	satlins: Symmetric saturating linear transfer function
		trainscg: Scaled conjugate gradient backpropagation	softmax: Soft max transfer function
			tansig: Symmetric sigmoid transfer function
			tribas: Triangular basis transfer function

for the number of layers, nodes, learning algorithms, and activation functions.

3.2.4 ANN-GA prediction results

Table 6 displays the experimental data of Ra that was used to develop the ANN model, as well as the corresponding predicted results of Ra obtained from the developed model.

Table 7 and Fig. 8 (spider plot) presents the values of different performance indices (PI) such as R, RSME, MAD, MAPE, and MAE of the surface roughness Ra model ANN model optimized by GA for the five (5) best iterations. These results show globally high IPs and particularly for the last iteration, where we observe very high IPs for learning, validation, and testing. The values of IP (R, RSME, MAD, MAPE, and MAE) of the learning are 0.9679, 0.5325, 0.9427, 10.52%, and 0.3633, respectively, indicating that the generated neural network is able to predict the roughness with great precision on the training data. For the validation and the test, the values of IP are 0.975, 1.3749, 1.4577, 23.71%, and 1.0696, which confirms that the neural network generalizes well on unknown data and able to accurately predict the values of Ra on new data. Finally, the global IP values are also high (0.9529, 0.665, 1.009, 11.84%, and 0.4339), suggesting that the neural network is able to accurately predict the surface roughness Ra in the dataset.

The graphical representation in Fig. 9 illustrates the comparison between the experimental (measured) values of Ra and the estimated values obtained by ANN-GA. Analysis of the figure reveals a strong correlation between the experimental values and the estimates generated by ANN-GA. This indicates the excellent capability of the ANN-GA model to capture the underlying relationship between the input variables and the corresponding output, Ra.

The achieved results provide compelling evidence that employing a genetic algorithm to optimize both the hyper parameters and architecture of the neural network has yielded remarkable performance in predicting surface roughness. However, it is crucial to emphasize that the quality of these results depends on the quality of the data used to train and validate the neural network.

The optimal ANN architectures for the best 5 iterations, selected based on their performance using the defined performance indices (IP), are presented in Table 8.

The results highlight the number of hidden layers, number of nodes in each layer, learning algorithm, and activation function employed to construct the neural network architectures with the best performance. Among these, the optimal architecture from the fifth iteration is characterized by the following parameter combination: three hidden layers, with 6, 7, and 3 nodes, respectively; the learning algorithm

Table 6 Experimental data versus predicted Ra using ANN

N°	*Ra Exp. (μm)*	*Ra ANN (μm)*	N°	*Ra Exp. (μm)*	*Ra ANN (μm)*	N°	*Ra Exp. (μm)*	*Ra ANN (μm)*	N°	*Ra Exp. (μm)*	*Ra ANN (μm)*
1	4.06	4.06	26	11.83	11.84	51	2.9	2.30	76	9.46	9.45
2	3.96	3.94	27	10.43	9.37	52	10.3	10.31	77	7.76	7.76
3	2.66	2.66	28	8.3	9.58	53	4.96	6.41	78	4.96	6.41
4	5.36	6.94	29	10.5	10.29	54	6.16	5.25	79	4.66	5.61
5	5.76	5.76	30	7.5	10.75	55	4.5	4.50	80	7.2	6.76
6	2.16	2.25	31	4.86	4.86	56	2.76	3.35	81	5.1	5.69
7	1.6	1.71	32	2.7	4.27	57	6.5	6.50	82	6.16	6.95
8	1.66	1.77	33	3	2.95	58	5.9	4.18	83	4.96	4.85
9	2.9	3.05	34	4.56	3.97	59	4.16	4.56	84	3.2	3.20
10	3.76	3.75	35	4.66	5.61	60	5.6	4.84	85	6	6.55
11	1.96	1.74	36	2.86	2.60	61	2.7	2.06	86	4.33	4.47
12	2.13	1.51	37	4.86	3.98	62	2.33	2.83	87	4.16	4.26
13	2.53	2.53	38	2.7	2.67	63	2.83	3.23	88	3.13	4.05
14	2	2.20	39	2.13	1.47	64	2.66	3.28	89	4.65	4.65
15	3.7	3.25	40	2.33	2.36	65	3.4	3.39	90	8.26	6.54
16	2.6	2.20	41	1.86	2.45	66	3.23	3.23	91	4.13	3.84
17	2.33	2.14	42	3.13	3.83	67	2.6	2.70	92	3.9	3.88
18	2.4	2.06	43	4.66	3.83	68	2.23	3.00	93	3.6	3.07
19	2.63	2.63	44	2.43	3.21	69	2.86	2.73	94	3.1	3.10
20	1.8	1.80	45	2.83	3.29	70	3	2.51	95	4.06	4.97
21	1.96	2.57	46	3.53	2.98	71	2.9	2.30	96	3.43	3.46
22	2.8	2.54	47	2.76	3.48	72	2.1	2.87	97	3.86	4.07
23	2.3	2.30	48	2.6	2.41	73	3.73	3.08	98	2.93	3.85
24	2.33	2.51	49	4.3	4.31	74	2.36	2.77	99	6.6	6.59
25	2.4	2.64	50	2.63	2.52	75	2.9	2.44	100	4.23	4.10

Table 7 ANN prediction errors

			5 Best Iterations				
		Optimal	1	2	3	4	5
R	Training	0.9679	0.9352	0.9473	0.9718	0.9165	0.9679
	Validation	0.9750	0.8881	0.9419	0.9441	0.9875	0.9750
	Test	0.9750	0.8881	0.9419	0.9441	0.9875	0.9750
	Global	0.9529	0.8989	0.9473	0.9254	0.8752	0.9529
RMSE	Training	0.5325	0.7168	0.7042	0.4932	0.8088	0.5325
	Validation	1.3749		0.4013	2.0992	2.8299	1.3749
	Test	1.3749	2.0400	0.4013	2.0992	2.8299	1.3749
	Global	0.6665	0.8670	0.6800	0.8122	1.1788	0.6665
MAD	Training	0.9427	0.4489	0.9333	0.9444	0.8818	0.9427
	Validation	1.4577	0.4489	1.1337	0.2566	1.8167	1.4577
	Test	1.4577	0.8126	1.1337	0.2566	1.8167	1.4577
	Global	1.009	0.1523	0.9380	0.8713	0.9692	1.0090
MAPE (%)	Training	10.52	19.51	15.33	10.71	16.27	10.52
	Validation	23.71	19.51	10	24.74	31.64	23.71
	Test	23.71	19.51	10	24.74	31.64	23.71
	Global	11.84	15.66	14.80	12.11	17.80	11.84
MAE	Training	0.3633	0.4825	0.5210	0.3152	0.5990	0.3633
	Validation	1.0696	1.1693	0.3319]	1.3155	1.5084	1.0696
	Test	1.0696	1.1693	0.3319]	1.3155	1.5084	1.0696
	Global	0.4339	0.5512	0.5021	0.4152	0.6900	0.4339

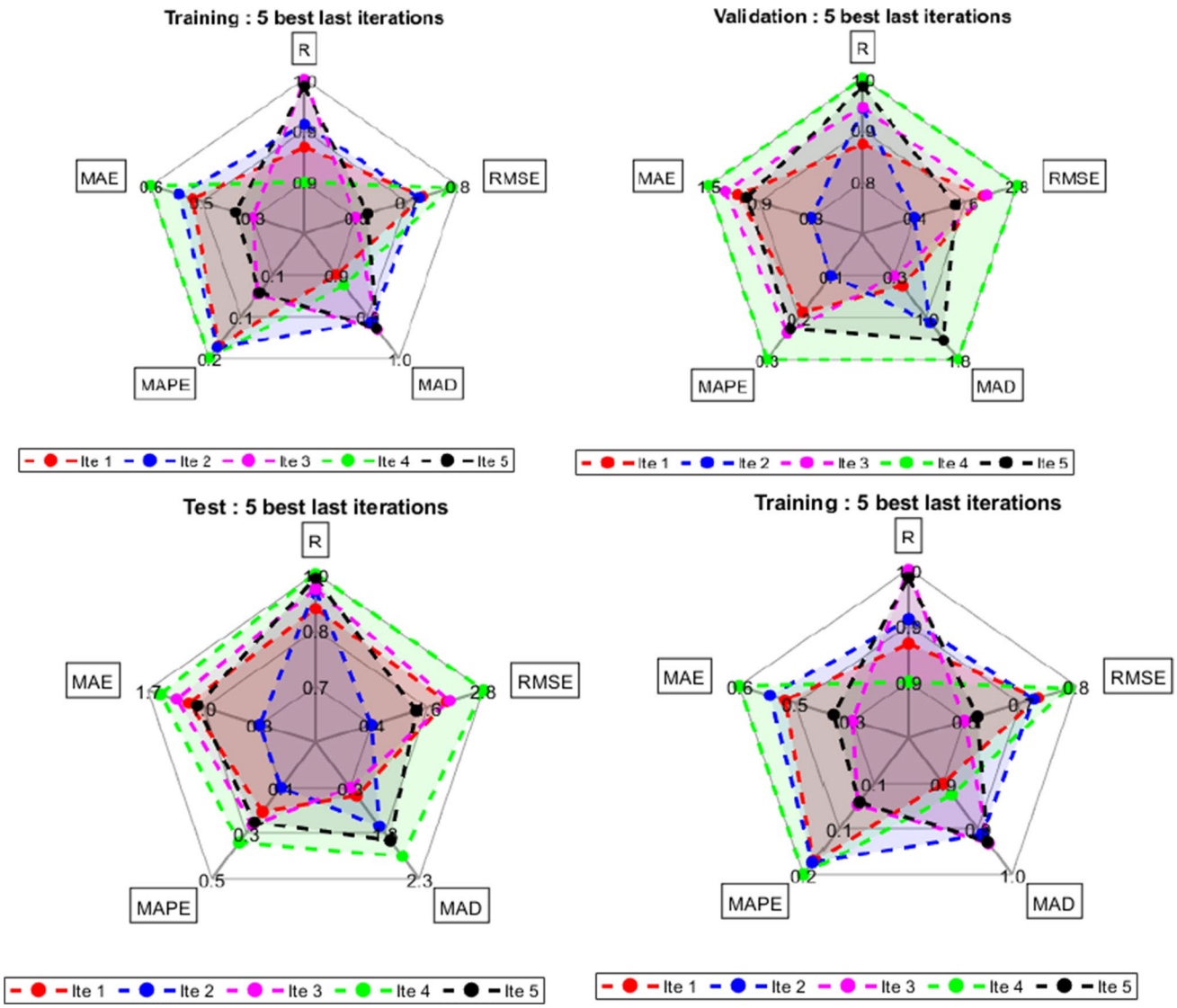

Fig. 8 Spider plot illustrating the performance indices for the top five iterations

trainbr; and activation functions tansig, radbasn, and netinv assigned to each respective layer.

3.2.5 Comparison between ANN-GA and LM algorithm

This section compares the neural network architecture discovered through genetic algorithms with the architectures employed in the Levenberg–Marquardt backpropagation (LM) algorithm. The LM algorithm is known for its proficiency in addressing nonlinear problems during the training of gradient backpropagation neural networks. It possesses the capability to locate local minima of the error function and exhibits faster convergence compared to traditional optimization methods like stochastic gradient descent. These findings offer insights into the predictive capabilities of the ANN-GA architectures obtained in this study.

The performance of the LM and ANN-GA neural network models is demonstrated through the results presented in Table 9 and the spider plots depicted in Fig. 10. The findings indicate that ANN-GA outperforms LM in terms of IP values. Consequently, these results suggest that employing a genetic algorithm for optimizing neural network architecture can be a highly effective approach for enhancing the predictive performance of neural network models.

4 Conclusion

This section provides a concise summary of the investigation conducted on surface roughness in Alfa/epoxy biocomposites. The focus of this research was to gain insights into the machining processes and surface quality of these

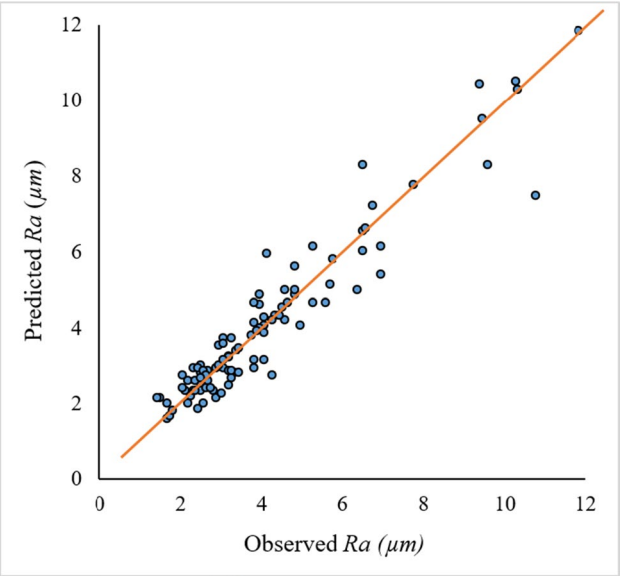

Fig. 9 Correlation between experimental Ra values and estimated values obtained by ANN-GA

environmentally friendly materials, with a particular emphasis on natural fiber-reinforced composites (NFRCs) as potential alternatives to conventional materials in various industries.

Table 8 Optimal ANN-GA architecture for the five best iterations

Iteration	HLayer number	HLayer size	Learning algorithm	Act-Fct
1	3	6	trainbr	tansig
		7		radbasn
		4		netinv
2	3	6	tansig	tansig
		7		radbasn
		3		netinv
3	3	6	trainbr	tansig
		7		radbasn
		3		netinv
4	3	6	trainlm	tansig
		7		radbasn
		3		netinv
5	3	6	trainbr	tansig
		7		radbasn
		3		netinv

Table 9 Comparison between ANN-GA and LM

IP global	AG OPT	LM (trainlm)
R	0.9529	0.8648
RMSE	0.6665	1.0707
MAD	1.009	0.9135
MAPE (%)	11.84	21.18
MAE	0.4339	

5 Key findings:

1. The analysis of variance (ANOVA) revealed that the feed per revolution and chemical treatment of fibers had significant impacts on surface roughness, while the effect of machining direction and the orientation of the fibers were relatively minor.
2. The hybrid ANN-GA (artificial neural networks-genetic algorithms) approach demonstrated superior predictive capabilities for surface roughness compared to the Levenberg–Marquardt backpropagation (LM) algorithm.
3. The developed ANN-GA model exhibited high accuracy in estimating surface roughness, as confirmed by the evaluation metrics used.

6 Implications

1. This study contributes to a deeper understanding of Alfa/epoxy biocomposites and their machining processes, shedding light on their unique properties and potential applications.
2. The identification of key factors influencing surface roughness provides valuable insights for optimizing the manufacturing processes of biocomposites, leading to improved product quality.
3. The successful application of the hybrid ANN-GA approach highlights its potential as an effective methodology for predicting surface roughness in NFRCs.
4. The findings of this study have implications for researchers and practitioners in industries such as automotive and aerospace, where the adoption of eco-friendly materials is gaining significance.

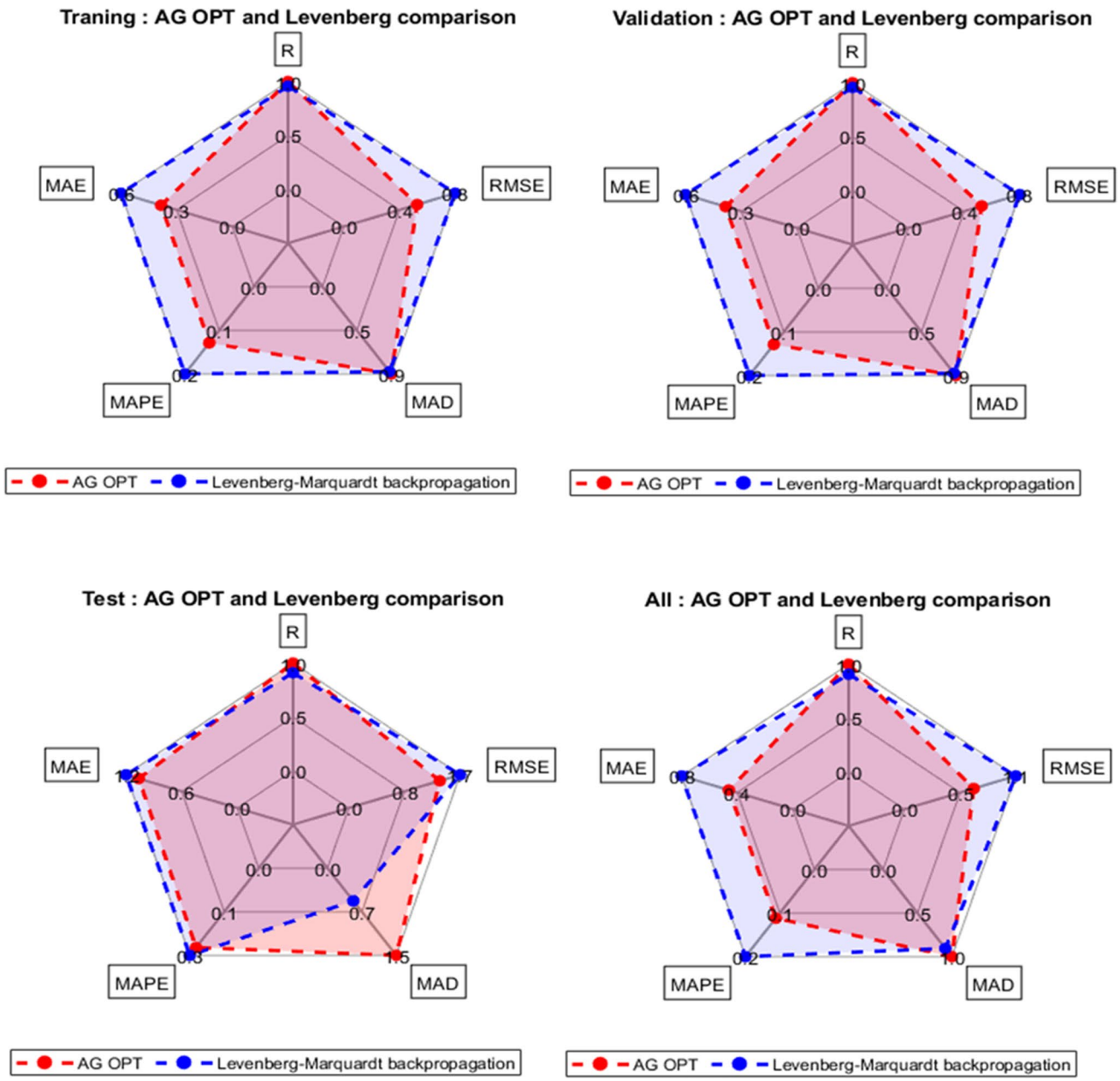

Fig. 10 Correlation between experimental data and estimated values using ANN-GA and LM

Finally, this research advances the knowledge in surface roughness analysis of Alfa/epoxy biocomposites and underscores the significance of eco-friendly materials for a sustainable future. The insights gained from this study open avenues for further advancements and broader applications in the field of natural fiber-reinforced composites.

Author contribution The paper was collaboratively authored by a team of individuals, each making unique contributions. MG conducted the literature study, experiments, and data analysis and also wrote the paper. MS acted as the project supervisor, providing the research idea, technical guidance, and ongoing support. He also participated in data analysis and took responsibility for finalizing the article. AL contributed to the modeling approach, while MA conducted the experiments. MR focused on the elaboration of composite materials. J-FC played a key role in the discussions and significantly contributed to the final draft of the article. All authors carefully reviewed and approved the final manuscript.

Funding This work was funded by the Ministry of Higher Education and Scientific Research of Algeria (MESRS) (grant # PRFU Project-N A11N01UN280120220003).

Data availability All data presented in this paper are available.

Code availability Can be made available upon request.

Declarations

Ethical approval Not applicable.

Consent to participate All authors contribute and participate in the work carried out in this paper.

Consent for publication The authors of this paper agree to publish this work in the *International Journal of Advanced Manufacturing Technology*.

Competing interests The authors declare no competing interests.

References

1. Behera RR et al (2016) Simultaneous prediction of delamination and surface roughness in drilling GFRP composite using ANN. Int J Plast Technol 20:424–450
2. Mohammed NH, Wolla DW (2022) Optimization of machining parameters in drilling hybrid sisal-cotton fiber reinforced polyester composites. AIMS Mater Sci 9(1):119–134. https://doi.org/10.3934/matersci.2022008
3. Sivam R (2009) Symposium on fibre reinforced composites, Port Elizabeth – South Africa 24 – 25 February
4. Lovins AB, Cramer DR (2004) Hypercars, hydrogen, and the automotive transition. Int J Veh Des 35(1–2):50–85
5. Chauhan V, Kärki T, Varis J (2022) Review of natural fiber-reinforced engineering plastic composites, their applications in the transportation sector and processing techniques. J Thermoplast Compos Mater 35(8):1169–1209
6. Christophe B (2013) Fibres naturelles de renfort pour matériaux composites. Éditions Techniques de l'Ingénieur 249. https://doi.org/10.51257/a-v3-am5130
7. Taallah B, Guettala A, Kriker A (2014) Effet de la teneur en fibres de palmier dattier et de la contrainte de compactage sur les propriétés des blocs de terre comprimée. Courrier du Savoir 18:45–51
8. Abdelaziz S et al (2013) Valorisation des tiges de dattiers dans la formulation des mortiers: propriétés physiques et mécaniques. AUGC, Mai 2013, LMT Cachan, France
9. Madhavan V et al (2015) Fiber orientation angle effects in machining of unidirectional CFRP laminated composites. J Manuf Process 20:431–442
10. Nayak D, Bhatnagar N, Mahajan P (2005) Machining studies of uni-directional glass fiber reinforced plastic (UD-GFRP) composites part 1: effect of geometrical and process parameters. Mach Sci Technol 9(4):481–501
11. Chakladar ND, Pal SK, Mandal P (2012) Drilling of woven glass fiber-reinforced plastic—an experimental and finite element study. Int J Adv Manuf Technol 58:267–278
12. Sorrentino L, Turchetta S (2014) Cutting forces in milling of carbon fibre reinforced plastics. Int J Manuf Eng 2014:439634. https://doi.org/10.1155/2014/439634
13. Li X, Tabil LG, Panigrahi S (2007) Chemical treatments of natural fiber for use in natural fiber-reinforced composites: a review. J Polym Environ 15:25–33
14. George M et al (2014) Characterization of chemically and enzymatically treated hemp fibres using atomic force microscopy and spectroscopy. Appl Surf Sci 314:1019–1025
15. El-Abbassi FE et al (2020) A review on alfa fibre (*Stipatenacissima* L.): From the plant architecture to the reinforcement of polymer composites. Compos Part A: Appl Sci Manuf 128:105677
16. Gares M, Hiligsmann S, KacemChaouche N (2020) Lignocellulosic biomass and industrial bioprocesses for the production of second generation bio-ethanol, does it have a future in Algeria? SN Appl Sci 2:1–19
17. Sun X-F et al (2013) Hemicellulose-based pH-sensitive and biodegradable hydrogel for controlled drug delivery. Carbohyd Polym 92(2):1357–1366
18. Zoghlami A, Paës G (2019) Lignocellulosic biomass: understanding recalcitrance and predicting hydrolysis. Front Chem 7:874
19. Kim S, Dale BE (2004) Global potential bioethanol production from wasted crops and crop residues. Biomass Bioenerg 26(4):361–375
20. Semhaoui I et al (2017) Bioconversion of Moroccan Alfa (Stipa Tenacissima) by thermomechanical pretreatment combined to acid or alkali spraying for ethanol production. J Mater 8:2619–2631
21. Labidi K et al (2019) Alfa fiber/polypropylene composites: influence of fiber extraction method and chemical treatments. J Appl Polym Sci 136(18):47392
22. Paiva M et al (2007) Alfa fibres: mechanical, morphological and interfacial characterization. Compos Sci Technol 67(6):1132–1138
23. Brahim BS, Cheikh RB, Baklouti M (2001) The alfa fibres in composite materials. In: Proceedings of ICCM-13 conference, 2001. ICCM, Beijing, China
24. Campos AR, Cunha AM, Cheikh RB (2003) Injection molding of a starch based polymer reinforced with natural fibres. In: Proceedings of SPE-ANTEC conference. SPE, Nashville, USA
25. Salim MH et al (2022) Alfa fibers, their composites and applications. Plant fibers, their composites, and applications. Elsevier, pp 51–74
26. Brahim SB, Cheikh RB (2007) Influence of fibre orientation and volume fraction on the tensile properties of unidirectional Alfa-polyester composite. Compos Sci Technol 67(1):140–147
27. Abdallah Y, Ben Cheikh R, Paiva M (2019) Could alfa fibers substitute glass fibers in composite materials? Int Polym Process 34(1):133–142
28. Bledzki A, Gassan J (1999) Composites reinforced with cellulose based fibres. Prog Polym Sci 24(2):221–274
29. Chafra M, Chevalier Y (2005) Directional damage and failure of composite materials under cyclic loading. Int J Veh Des 39(1–2):163–172
30. Zrida M, Laurent H, Rio G (2016) Numerical study of mechanical behaviour of a polypropylene reinforced with Alfa fibres. J Compos Mater 50(21):2883–2893
31. Arrakhiz F et al (2012) Mechanical and thermal properties of polypropylene reinforced with Alfa fiber under different chemical treatment. Mater Des 35:318–322
32. Rajesh M, Kandasamy J, Mallikarjuna Reddy D, Mugeshkannan V, Kar VR (2021) Experimental Characterization for Natural Fiber and Hybrid Composites. In: Jawaid M, Hamdan A, Hameed Sultan MT (eds) Structural Health Monitoring System for Synthetic, Hybrid and Natural Fiber Composites. Composites Science and Technology. Springer, Singapore. https://doi.org/10.1007/978-981-15-8840-2_6
33. Benyamina B et al (2021) Study and modeling of thermomechanical properties of jute and Alfa fiber-reinforced polymer matrix hybrid biocomposite materials. Polym Bull 78:1771–1795
34. El-Abbassi FE et al (2015) Effect of alkali treatment on Alfa fibre as reinforcement for polypropylene based eco-composites: Mechanical behaviour and water ageing. Compos Struct 133:451–457
35. Chegdani F, Mezghani S, El Mansori M (2016) On the multiscale tribological signatures of the tool helix angle in profile milling of woven flax fiber composites. Tribol Int 100:132–140

36. Chegdani F et al (2020) Effect of flax fiber orientation on machining behavior and surface finish of natural fiber reinforced polymer composites. J Manuf Process 54:337–346
37. Kumaran ST et al (2017) Prediction of surface roughness in abrasive water jet machining of CFRP composites using regression analysis. J Alloy Compd 724:1037–1045
38. John R et al (2021) Effects of machining parameters on surface quality of composites reinforced with natural fibers. Mater Manuf Processes 36(1):73–83
39. Vinayagamoorthy R, Rajeswari N (2012) Analysis of cutting forces during milling of natural fibered composites using fuzzy logic. Int J Compos Mater Manuf 2(3):15–21
40. Babu GD, Babu KS, Gowd BUM (2013) Effect of machining parameters on milled natural fiber-reinforced plastic composites. J Adv Mech Eng 1(1):1–12
41. bin Harun A et al (2015) Study the effect of milling parameters on surface roughness during milling kenaf fibre reinforced plastic. Adv Environ Biol 9(13):46–53
42. Benyettou R, Amroune S, Slamani M, Kiliç A (2023) Investigation of machinability of biocomposites: modeling and ANN optimization. Academic J Manuf Eng 21(1):97–104
43. Tran DS et al (2020) Effects of reinforcements and cutting parameters on machinability of polypropylene-based biocomposite reinforced with biocarbon particles and chopped miscanthus fibers. Int J Adv Manuf Technol 110:3423–3444
44. Tran DS, Songmene V, Ngo AD (2021) Regression and ANFIS-based models for predicting of surface roughness and thrust force during drilling of biocomposites. Neural Comput Appl 33:11721–11738
45. Belaadi A et al (2022) Drilling performance prediction of HDPE/Washingtonia fiber biocomposite using RSM, ANN, and GA optimization. Int J Adv Manuf Technol 123(5–6):1543–1564
46. Nouioua M et al (2022) Evaluation of: MOSSA, MOALO, MOVO and MOGWO algorithms in green machining to enhance the turning performances of X210Cr12 steel. Int J Adv Manuf Technol 120(3–4):2135–2150
47. Benyahia A, Merrouche A, Rokbi M, Kouadri Z (2013) Study the effect of alkali treatment of natural fibers on the mechanical behavior of the composite unsaturated Polyester-fiber Alfa. Composites 2(3):69–73
48. Laouissi A et al (2021) Machinability study and ANN-MOALO-based multi-response optimization during Eco-Friendly machining of EN-GJL-250 cast iron. Int J Adv Manuf Technol 117(3–4):1179–1192
49. Laouissi A et al (2019) Investigation, modeling, and optimization of cutting parameters in turning of gray cast iron using coated and uncoated silicon nitride ceramic tools. Based on ANN, RSM, and GA optimization. Int J Adv Manuf Technol 101(1–4):523–548
50. Muoi PQ et al (2016) Descent gradient methods for nonsmooth minimization problems in ill-posed problems. J Comput Appl Math 298:105–122
51. Senov A, Granichin O (2017) Projective approximation based gradient descent modification. IFAC-PapersOnLine 50(1):3899–3904
52. Singh BK, Verma K, Thoke A (2015) Adaptive gradient descent backpropagation for classification of breast tumors in ultrasound imaging. Procedia Comput Sci 46:1601–1609
53. Møller MF (1993) A scaled conjugate gradient algorithm for fast supervised learning. Neural Netw 6(4):525–533
54. Moré JJ (1978) The Levenberg-Marquardt algorithm: implementation and theory. In: Watson GA (eds) Numerical Analysis. Lecture Notes in Mathematics, vol 630. Springer, Berlin, Heidelberg. https://doi.org/10.1007/BFb0067700
55. Sun Z et al (2017) A Bayesian regularized artificial neural network for adaptive optics forecasting. Opt Commun 382:519–527
56. Heydecker BG, Wu J (2001) Identification of sites for road accident remedial work by Bayesian statistical methods: an example of uncertain inference. Adv Eng Softw 32(10–11):859–869
57. Laouissi A et al (2022) Heat treatment process study and ANN-ga based multi-response optimization of C45 steel mechanical properties. Met Mater Int 28(12):3087–3105